Acta Diabetologica (2019) 56:1265–1274
https://doi.org/10.1007/s00592-019-01382-x

ORIGINAL ARTICLE

Timp3 deficiency affects the progression of DEN-related hepatocellular carcinoma during diet-induced obesity in mice

Viviana Casagrande[1,2,3] · Alessandro Mauriello[4] · Lucia Anemona[4] · Maria Mavilio[1] · Giulia Iuliani[1] · Lorenzo De Angelis[1] · Mara D'Onofrio[5,6] · Ivan Arisi[5,6] · Massimo Federici[1] · Rossella Menghini[1]

Received: 20 April 2019 / Accepted: 15 June 2019 / Published online: 10 July 2019

Abstract

Aim Obesity and low-grade inflammation are associated with an increased risk of hepatocellular carcinoma (HCC), a leading cause of cancer-related death worldwide. The tissue inhibitor of metalloproteinase (TIMP) 3, an endogenous inhibitor of protease activity that represents a key mediator of inflammation, is reduced in inflammatory metabolic disorders and cancer. In contrast, Timp3-deficient mice ($Timp3^{-/-}$) are highly resistant to developing HCC in response to a diethylnitrosamine (DEN); therefore, we aimed to elucidate the biological role of genetic loss of Timp3 in obesity-related hepatocarcinogenesis.

Methods Fourteen-day-old male wild-type (wt) and $Timp3^{-/-}$ mice were injected with 25 mg/kg DEN or an equal volume of saline. After 4 weeks, mice were randomized into two dietary groups and fed either normal or high-fat diet and allowed to grow until 32 weeks of age. Liver histological features were analyzed, and differentially expressed genes in the liver were quantified.

Results In $Timp3^{-/-}$ mice fed with the obesogenic diet, despite the increase in liver steatosis and inflammation, both the number of tumors and the total tumor size are significantly reduced 30 weeks post-DEN injection, compared to control mice. Moreover, Timp3 deletion in hepatocarcinogenesis during obesity is associated with a reduction in FoxM1 transcriptional activity through H19/miR-675/p53 pathway.

Conclusions This study suggests that Timp3 ablation leads to cell cycle perturbation, at least in part by repressing FoxM1 transcriptional activity through H19/miR-675/p53 pathway.

Keywords Hepatocellular carcinoma · Obesity · TIMP3 · Inflammation

Introduction

Obesity and type 2 diabetes pandemics are associated with an increased prevalence of complications including cancer [1]. Hepatocellular carcinoma (HCC) is a complication of chronic liver disease, and it is the sixth cause of cancer-related death in the world [1]. Recent epidemiological and experimental studies have revealed that an increasing

Managed by Antonio Secchi.

Electronic supplementary material The online version of this article (https://doi.org/10.1007/s00592-019-01382-x) contains supplementary material, which is available to authorized users.

✉ Rossella Menghini
menghini@med.uniroma2.it

[1] Department of Systems Medicine, University of Rome Tor Vergata, Via Montpellier, 1, 00133 Rome, Italy

[2] Research Unit of Diabetes and Endocrine Diseases and 2 Unit of Biostatistics, Fondazione IRCCS "Casa Sollievo della Sofferenza", San Giovanni Rotondo, Italy

[3] Unit of Biostatistics, Fondazione IRCCS "Casa Sollievo della Sofferenza", San Giovanni Rotondo, Italy

[4] Department of Biomedicine and Prevention, University of Rome Tor Vergata, 00133 Rome, Italy

[5] European Brain Research Institute (EBRI) "Rita Levi-Montalcini", 00161 Rome, Italy

[6] Institute of Translational Pharmacology (IFT), CNR, 00133 Rome, Italy

number of HCC cases are associated with obesity, type 2 diabetes (T2D) and related metabolic diseases, such as non-alcoholic steatohepatitis (NASH) [2, 3]. TIMP3 is a 24–27-kDa protein belonging to the family of TIMPs that binds to the extracellular matrix and participates in the modulation of inflammation, in cellular migration and in proliferation [4]. In addition to inhibiting MMPs, TIMP3 is also an efficient inhibitor of multiple members of the a disintegrin and metalloproteinase (ADAM) domain family, including ADAM17. Previous reports have implicated the ADAM17/TIMP3 dyad as a mediator in the development and progression of non-alcoholic fatty liver disease (NAFLD) [5–7]. Recent studies have identified Timp3 as a potential tumor suppressor gene involved in the induction of tumor cell apoptosis, prevention of tumor, extracellular matrix (ECM) remodeling and inhibition of tumor-derived angiogenic activity [8, 9].

Interestingly, Timp3 is down-regulated in liver and adipose tissue in both genetic and nutritional models of obesity in mice, as well as in patients with obesity-related T2D [7, 10, 11], and the combination of Timp3 ablation with environmental stress (high-fat diet) impacts on inflammation, liver steatosis and fibrosis, resulting in a phenotype similar to NASH [5, 10]. Moreover, in a mouse model of diethylnitrosamine (DEN)-induced liver tumorigenesis, which recapitulates human HCC with poor prognosis [12], combined with dietary-induced obesity, specific hepatocellular Timp3 overexpression dampened HCC progression [13].

On the other hand, recent evidence shows that genetic loss of Timp3 in liver protects from carcinogen-induced HCC through the immediate engagement of several tumor suppressor pathways including apoptosis and senescence [14].

In this study, we investigated therefore which prevalent liver phenotype results from the combination of diet-induced obesity and carcinogen-induced HCC in Timp3 knockout mice.

Materials and methods

Mice and treatments

Timp3$^{-/-}$ mice on a C57BL/6 background, as well as the metabolic testing procedures, have been previously described [4, 5]. The handling of mice and experimental procedures were conducted in accordance with experimental animal guidelines. Animal studies were approved by the University of Tor Vergata Animal Care and Use Committee.

For long-term experiment, male mice were injected intraperitoneally with 25 mg/kg body weight of DEN (Sigma-Aldrich, St. Louis, MO, USA) at the age of 2 weeks, whereas littermate controls were injected with an equal volume of saline. After 4 weeks, mice were separated into two dietary groups and fed either normal (10% calories from fat; Mucedola s.r.l., Settimo Milanese, Italy) or high-fat diet (60% of calories from fat; Research Diets, New Brunswick, NJ, USA) and allowed to grow until 32 weeks of age.

Analysis of liver tumor

Mice were killed for examination of liver tumors after overnight starvation. Unbroken livers were removed, weighed and photographed with a measuring scale. Tumors on the liver surface of each mouse were counted and measured by vernier caliper.

Liver histological lesions were classified according to standardized and internationally accepted nomenclature for classification of rodent tumors by two different experienced pathologists in a blind fashion [15].

ADAM17 activity

ADAM17 activity was determined using the SensoLyte 520 TACE Activity Assay Kit (AnaSpec, San Jose, CA, USA), in accordance with the manufacturer's protocol [13].

RNA microarray and gene expression analysis

A whole-genome microarray analysis (SurePrint G3 Unrestricted Gene Expression 8 × 60 K Microarray, Agilent platform) was performed on RNA extracted from liver tissue of wt and Timp3$^{-/-}$ DEN/HFD mice ($n = 3$ per group), according to the manufacturer's instructions. Agilent Microarray scanner G2564C was used for slide acquisition, and spot analysis was performed with Feature Extraction software (Agilent).

Data filtering and analysis were performed using R/Bioconductor and Microsoft Excel. Differentially expressed genes (DEGs) were selected by a combination of fold change and moderated t test thresholds (R Limma test p value < 0.05; |Log2 foldchange| > 2.0). DEGs lists were used for biological pathways and network analysis. Gene ontology (GO)-biological process hierarchy and Reactome pathway enrichment analysis were performed by using the PANTHER database (Protein ANalysis THrough Evolutionary Relationships, http://pantherdb.org) [16].

The protein–protein interaction (PPI) networks of DEGs were constructed using the Search Tool for the Retrieval of Interacting Genes (STRING, http://string-db.org) database and were visualized using Cytoscape 3.6 software (http://www.cytoscape.org/index.html). The DEGs were mapped into PPIs, and a combined score of > 0.4 was set as a threshold value in this study. Moreover, the nodes with higher degrees of interaction were considered as hub nodes. Hub gene sets obtained from the PPI network were used as input gene sets for sub-network construction.

RNA, microRNA isolation and gene expression analysis

Total RNA was isolated from liver tissue using TRIzol reagent (Life Technologies Corporation, CA, USA). A quantitative real-time PCR (RT-PCR) was performed as previously reported [13].

Enriched miRNA was isolated from liver tissue with the mirVana miRNA Isolation Kit (Ambion Inc., Austin, Tex); real-time quantification to measure miRNAs was performed as previously reported [17].

Immunoblotting

Western blots were performed on total tissue homogenates prepared as previously described [5]. The following antibodies were used: anti-phospho-Tyr705 STAT3, total STAT3, actin and p53 (Cell Signaling Technology, Danvers, MA).

Statistical analysis

Results of the experimental studies are expressed as mean ± standard error of the mean (SEM). Statistical analyses were performed using GraphPad Prism (v.5.02). Groups were compared using a two-tailed unpaired Student's t test or one-way ANOVA with Bonferroni' multiple comparison test or with Dunnett's multiple comparison test as indicated. Values of $p < 0.05$ were considered to be statistically significant.

Results

Timp3 genetic deletion protects from DEN-induced HCC during obesity

To determine the role of Timp3 deletion in hepatocarcinogenesis during obesity, 14-day-old male wild-type (wt) and Timp3$^{-/-}$ mice were injected with 25 mg/kg DEN [15] and 4 weeks later they were placed on either high-fat diet (HFD), in which 60% of calories are fat derived, or a normal diet (ND) containing 10% calories from fat, as a control. At 7 months of age, mice maintained on HFD gained more weight than mice on ND and their relative liver weight was increased (Fig. 1a). However, Timp3$^{-/-}$ on HFD displayed a lower liver/body weight ratio and higher blood glucose levels (Fig. 1a). Moreover, as expected, a disintegrin and a metalloproteinase (ADAM) 17 activity in liver tissue was increased in all Timp3$^{-/-}$ mice, compared to the wt control group (Fig. 1b). By contrast, serum levels of IL-6 and TNF-α were similar between wt and Timp3 null mice (Fig. 1c).

All mice given DEN developed typical HCC (Fig. 2). The multiplicity and total size of tumors were significantly higher in mice kept on HFD than in ND mice in both wt and Timp3$^{-/-}$ groups, confirming that obesity may contribute to the HCC development in mice [18] (Fig. 2). However, independent of diet conditions, the number of detectable tumors and total tumor size were significantly higher in wt mice than in Timp3$^{-/-}$ mice.

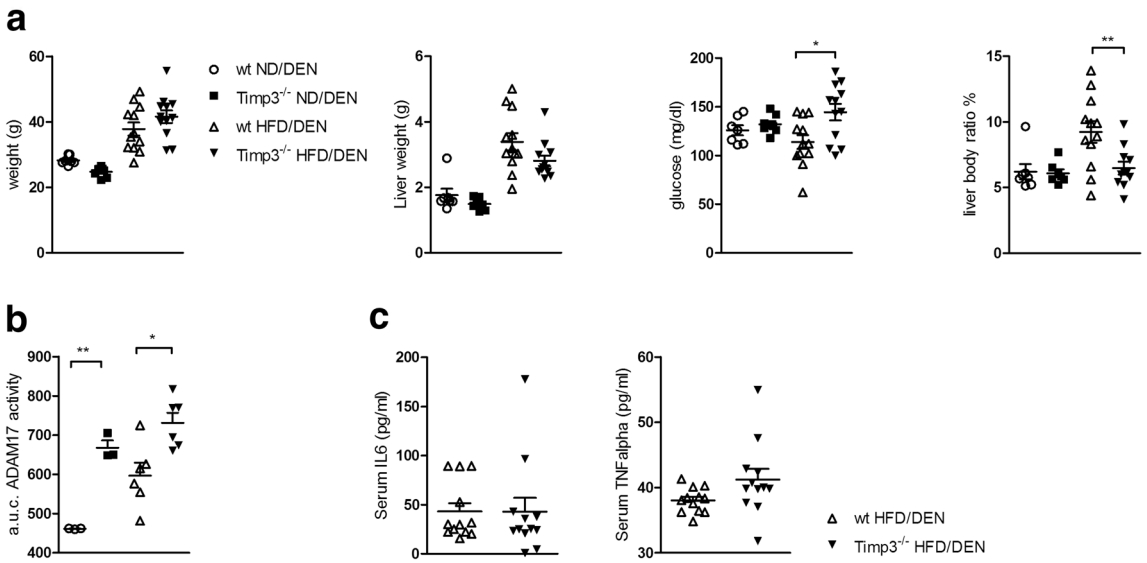

Fig. 1 Metabolic effect in 32-week-old lean and obese mice treated with DEN at 2 weeks of age. **a** Total body weight, liver weight, blood glucose levels and liver weight as a percentage of total body weight (ND $n=7$ HFD $n=12$ per group; data are mean ± SEM, one-way ANOVA with Bonferroni multiple comparison test). **b** ADAM17 activity (a.u.c. = area under the curve) measured in ND and HFD mice liver tissue (ND $n=3$ HFD $n=6$ per group; data are mean ± SEM, one-way ANOVA with Bonferroni multiple comparison test). **c** Serum levels of IL-6 and TNF-α ($n=12$ per group; values are represented as mean ± SEM, Student's t test). $^{*}p < 0.05$; $^{**}p < 0.01$

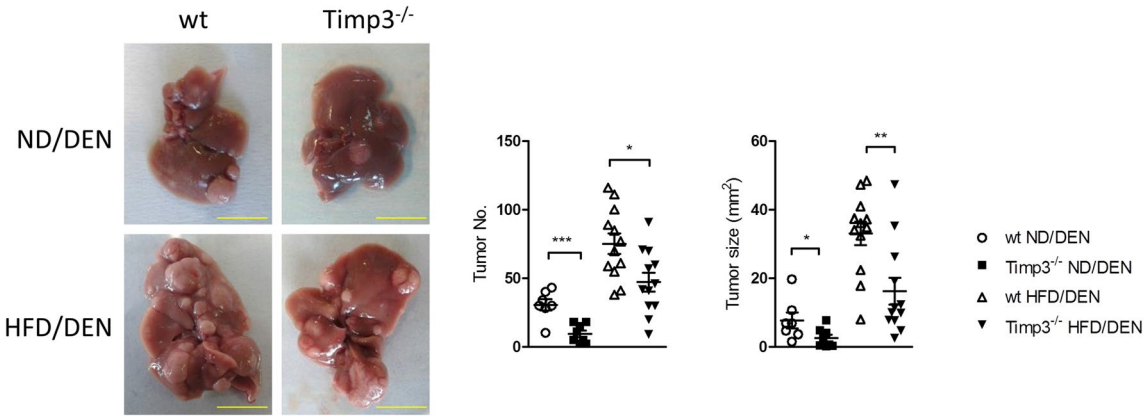

Fig. 2 DEN-induced HCC development in lean and obese mice. Livers of male wt and Timp3$^{-/-}$ mice kept on normal diet (ND) or high-fat diet (HFD) from week 6 to week 32 after the administration of DEN (25 mg/kg) at 2 weeks of age. Scale bars, 1 cm. Quantification of macroscopic tumor multiplicity and size determined by visual inspection in livers of DEN-injected wt and Timp3$^{-/-}$ male mice kept on ND or HFD. ND $n=7$ HFD $n=12$ per group; data are mean ± SEM, one-way ANOVA with Bonferroni multiple comparisons test; *$p<0.05$; **$p<0.01$; ***$p<0.0005$

HCC displays different histological characteristics in DEN-treated wt and Timp3$^{-/-}$ mice

Necroscopy observation clearly showed a reduced presence of tumors in Timp3$^{-/-}$ mice. Therefore, we performed a histological assessment in both peritumoral and intratumoral areas and quantified several featured associated with steatosis, inflammation, necrosis and intracellular abnormalities such as Mallory bodies (Fig. 3). In parenchymal area, wt and Timp3$^{-/-}$ mice treated with DEN showed similar characteristics, whereas Timp3$^{-/-}$ mice under the combined DEN/HFD regimen showed increased steatosis compared with wt. An analysis of tumoral tissue revealed no difference in steatosis but higher inflammation and Mallory bodies presence in Timp3$^{-/-}$ compared with wt mice.

Identification of differentially expressed genes (DEGs) in HCC during obesity

To evaluate the impact of Timp3 deletion on gene expression profile, microarray analysis was conducted on liver RNA from DEN-treated wt and Timp3$^{-/-}$ mice on HFD ($n=3$ for each group). Differential expression analysis revealed that 190 genes were significantly up-regulated and 456 down-regulated (fold change > 2 and p value < 0.05) in Timp3$^{-/-}$ liver mice in comparison with wt. Gene ontology-biological process (GO-BP) functional analysis and Reactome pathway enrichment analysis were performed for DEGs (Fig. 4a).

The top three enriched GO terms in the BP category included mitotic cell cycle process ($p=3.30\times10^{-5}$), involving DEGs, such as Sgol1, Cdkn3, Birc5, Cdkn2B, alpha amino acid ($p=3.3\times10^{-5}$) and fatty acid biosynthetic process ($p=1.6\times10^{-6}$) associated with DEGs, such as Psat1, Asns, Phgdh, Elovl7, Cyp39a1 and Scd2 (Fig. 4a, upper panel).

Moreover, the Reactome pathway enrichment analysis showed a list of metabolic pathways enriched in Timp3$^{-/-}$ liver mice, including "Extracellular matrix organization" and "TP53 Regulates Transcription of Cell Cycle Genes" (Fig. 4a, lower panel).

A list of the top 15 most significantly up- or down-regulated DEGs indicated that ablation of Timp3 expression affects a characteristic HCC expression profile including oncofetal genes, such as H19 (the most down-regulated among the whole analyzed genes), Afp, Lys6d and Gpc3 (Fig. 4b).

Additionally, a protein–protein interaction (PPI) information of DEGs was acquired from Search Tool for the Retrieval of Interacting Genes (STRING) database, and a PPI network was constructed using Cytoscape software. The obtained core sub-network from the PPI network included 43 DEGs (Fig. 4c). It is noteworthy that a number of DEGs exhibited degrees > 10, including Forkhead box M1 (FoxM1), and DEGs involved in FoxM1-related senescence such as cyclin-dependent kinase 1 (Cdk1), Kif20A, Aurora A kinase (Aurka), polo-like kinase 1 (Plk1), Cdkn2b, CenPA and Nek2.

Timp3 genetic deletion inhibits H19 expression during hepatocarcinogenesis

The 2.3-kb-long noncoding RNA H19 represents the most differentially expressed gene in microarray analysis; therefore, the expression levels of H19 were validated by quantitative RT-PCR in a larger sample size ($n=12$ for each

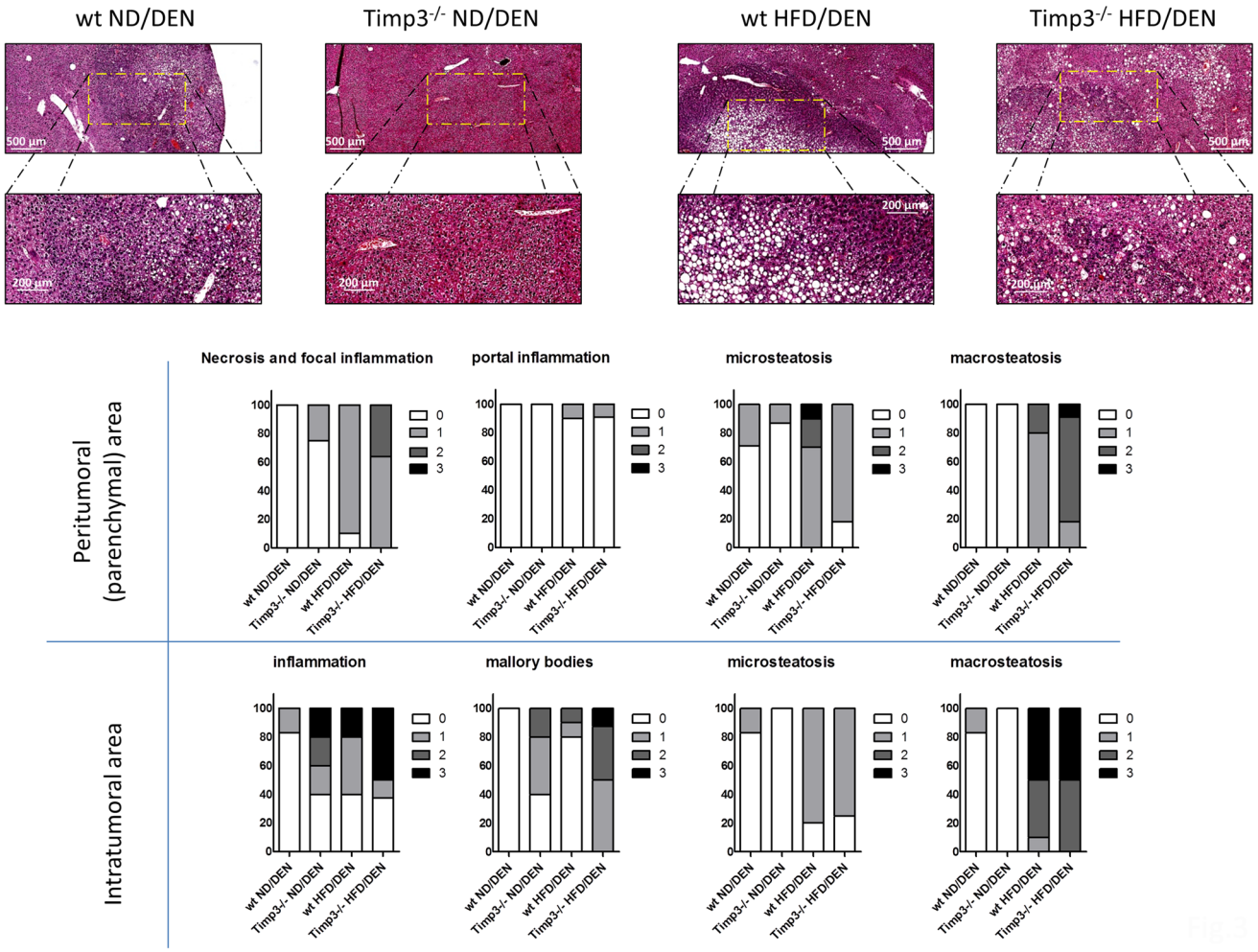

Fig. 3 Histopathological evaluations of livers in DEN-treated 32-week-old wt and Timp3$^{-/-}$ mice kept on ND or HFD. Representative images of liver sections stained with hematoxylin and eosin (H&E). Scale bars are indicated. Quantification of featured associated with DEN-induced HCC in both peritumoral and intratumoral areas. Numerical grading was performed using Ishak's scoring system. ND $n=7$, HFD $n=12$ per group

group). RT-PCR analysis confirmed that after DEN treatment, hepatic H19 levels were significantly down-regulated in liver of Timp3$^{-/-}$ mice fed a HFD, compared to wt HFD mice (Fig. 5a). In different cells, several cancer-promoting effects of H19 were delivered via microRNA-675 (miR-675), a short noncoding RNA transcribed from the first exon of H19 [19]. Consistent with H19 results, miR-675 expression was significantly lower in Timp3$^{-/-}$ HFD mice, compared to wt HFD mice (Fig. 5b).

p53 expression is induced in DEN-treated Timp3$^{-/-}$ mice fed a HFD

MiR-675 has a major role in inhibiting protein expression of p53, a crucial tumor suppressor gene in cancer [20, 21]. Protein levels of p53 were significantly suppressed in wt HFD mice treated with DEN, compared to Timp3$^{-/-}$ (Fig. 5c). Moreover, phosphorylation of STAT3, which was reported to be down-regulated by p53 [22], was suppressed in Timp3$^{-/-}$ mice, whereas the expression level of STAT3 was unaltered in comparison with the control (Fig. 5d), suggesting that STAT3 signal transduction, activated by phosphorylation, was reduced in the Timp3$^{-/-}$ model.

It is to be noted that the PPI network analysis identified FoxM1 as a node with a high degree of interaction (Fig. 5e). FoxM1, an essential transcription factor which has been reported to play important roles in the pathogenesis and progression of many human cancers, including HCC, is down-regulated by p53 [23].

To confirm the effect of Timp3 genetic deletion on FoxM1 pathway expression, the relative mRNA levels of FoxM1 and its downstream genes were examined using RT-PCR. The mRNA expression of FoxM1, Aurka and Plk1 was markedly reduced compared with control mice (Fig. 5f). Several

a

GO biological process complete	Fold Enrichment	raw P value	FDR
mitotic cytokinesis	7.32	3.33E-05	1.77E-02
alpha-amino acid biosynthetic process	6.25	3.31E-05	1.82E-02
fatty acid biosynthetic process	5.81	1.26E-06	1.50E-03
mitotic spindle organization	5.33	1.01E-04	3.78E-02
mitotic cell cycle phase transition	4.66	5.33E-06	4.82E-03
unsaturated fatty acid metabolic process	4.63	1.23E-04	4.29E-02
mitotic nuclear division	3.99	5.04E-05	2.15E-02

b

GeneSymbol	logFC	adj.P.Val
H19	-7,23	2,07E-02
Tceal5	-5,46	5,12E-02
Tspan8	-5,19	8,81E-02
Kif5c	-5,04	1,24E-01
Afp	-4,97	1,09E-01
Asns	-4,55	1,21E-01
Tff3	-4,47	6,40E-02
Bex1	-4,43	1,31E-01
Cdkn2b	-4,26	1,73E-01
Scd2	-4,22	4,55E-02
Spink3	-4,01	1,76E-01
Ly6d	-4	2,03E-02
Phgdh	-3.85	1.73E-01
Akr1c18	-3.8	1.86E-01
Gpc3	-3.53	1.37E-01

c

Reactome pathways	Fold Enrichment	raw P value	FDR
G2/M DNA replication checkpoint	24.15	7.24E-04	4.57E-02
Regulation of IGF transport and uptake by IGFBPs	16.1	2.08E-10	3.15E-07
Amino acid synthesis and interconversion (transamination)	12.25	5.93E-06	1.80E-03
Cyclin A/B1 associated events during G2/M transition	10.98	4.72E-05	5.95E-03
Regulation of cholesterol biosynthesis by SREBP (SREBF)	9.09	3.11E-05	5.23E-03
TP53 Regulates Transcription of Cell Cycle Genes	7.79	2.42E-04	1.93E-02
Activation of Matrix Metalloproteinases	7.55	8.64E-06	2.18E-03
Fatty Acyl-CoA Biosynthesis	7	4.42E-05	6.08E-03

d

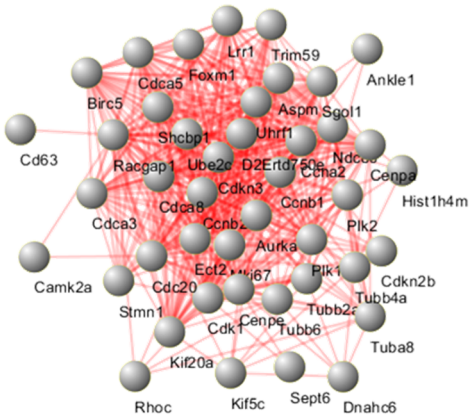

Fig. 4 Bioinformatic analysis of differentially expressed genes between DEN-treated wt and Timp3$^{-/-}$ mice fed HFD (DEN/HFD). **a** PANTHER was used to perform gene ontology-biological process (GO) and Reactome pathway enrichment analysis. **b** The top 15 differentially down-regulated genes in Timp3$^{-/-}$ DEN/HFD mice compared to wt DEN/HFD mice. **c** A protein–protein interaction network was established using STRING and Cytoscape. In the graphical representation of the molecular connectivity between proteins, the core network displays 43 gene products. wt and Timp3$^{-/-}$ DEN/HFD $n=3$ per group

genes that were modulated in tumor tissues (H19, FoxM1, Aurka, Plk1, Cdk1, Cdkn2b, Scd2) and protein expression of p53 were then analyzed in tumor–adjacent non-tumor tissues (Supplementary Fig. 1). The obtained results indicate that the modulation is restricted to tumor tissue.

Discussion

Obesity was recognized as a major risk factor for several common types of cancer, with the highest increased risk in liver cancer (HCC) [24]. The connection between obesity and cancer is explained partially by a state of chronic low-grade inflammation caused by elevated production of inflammatory cytokines [25]. TIMP3 is considered a tumor suppressor, as its expression is silenced through different mechanisms, in several malignant tumors [26]. Moreover, the decrease in Timp3 induced during obesity modifies the inflammatory scenario within the liver, promoting both hepatic steatosis and stromal cells activation, a step that could promote a pro-tumor microenvironment [5]. Since genetic loss of metalloproteinase inhibitor Timp3 delays hepatic tumorigenesis [14], here we evaluated the impact of Timp3 deletion, which exacerbates the detrimental response to HFD, during obesity-related HCC. Surprisingly, despite the increased steatosis in parenchymal liver tissue, Timp3 deletion reduced also susceptibility to HCC during obesity. However, both inflammatory response and Mallory bodies presence increased in intratumoral areas of Timp3 null mice. This suggests that the immune network induced by DEN and HFD, including infiltration of macrophages and release of immune factors, could be more efficient in fighting cellular stresses in tumors. This effect is consistent with the evidence that Timp3 null macrophages exhibited an increased proinflammatory (M1) phenotype in vitro [27].

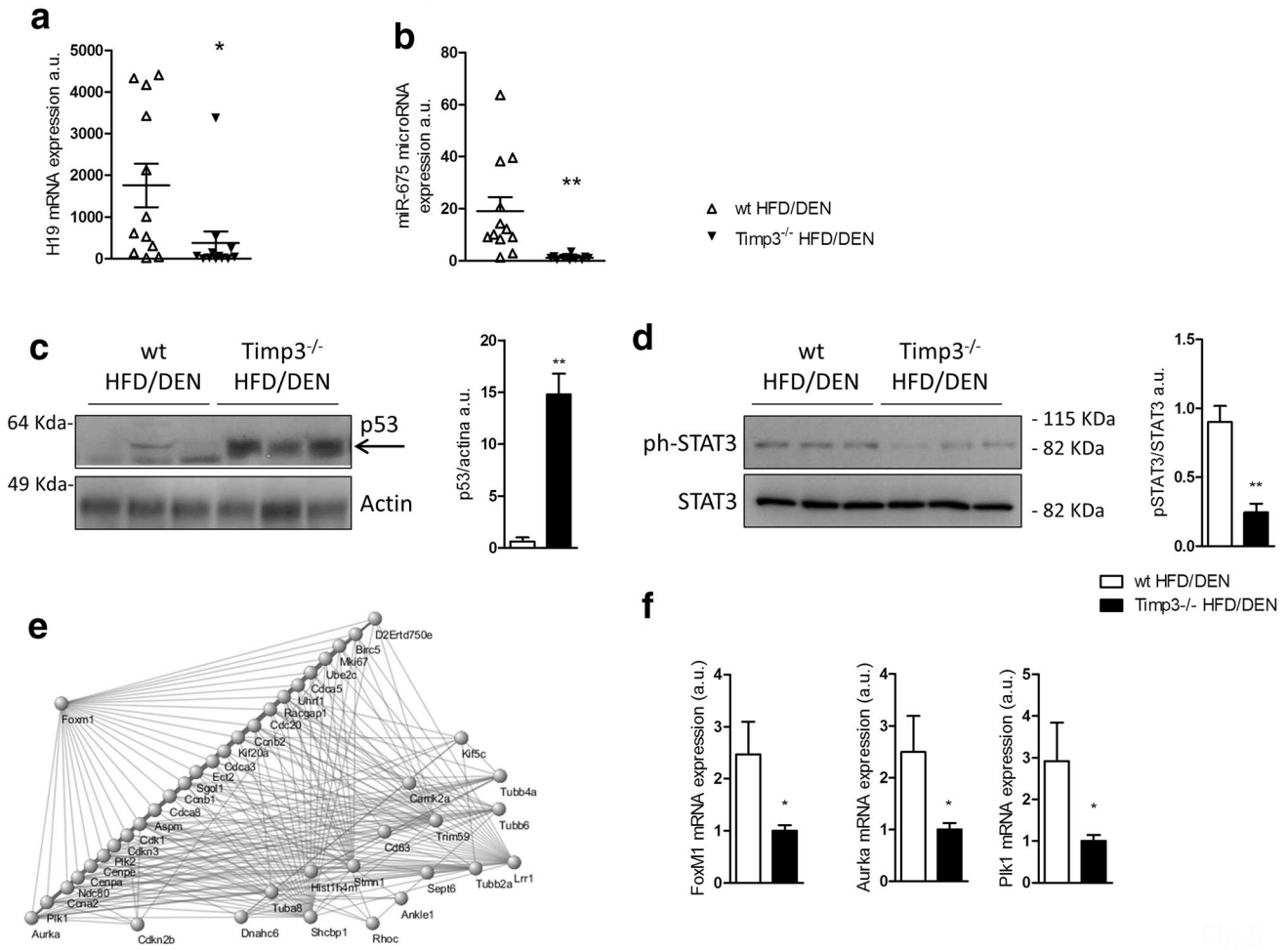

Fig. 5 Knockout of Timp3 down-regulates the expression of the long noncoding RNA H19 after DEN-induced hepatic injury, while p53 protein levels are significantly increased. **a**, **b** mRNA expression of H19 and miR-675 determined by RT-PCR in DEN-treated 32-week-old mice fed a HFD. ($n=12$ per group). **c**, **d** Livers were analyzed for p53 (normalized to β-actin) and phospho-STAT3 (normalized to STAT3) in total extract by Western blot ($n=12$ per group). **e** Graphical representation (Cytoscape software) of the molecular connectivity between FoxM1 and its major interacting proteins ($n=3$ per group). **f** RT-PCR analysis (normalized to β-actin) of FoxM1 and its target genes Aurka and Plk1 in wt and Timp3$^{-/-}$ mice ($n=12$ per group). Values are represented as mean ± SEM, Student's t test, $^{*}p<0.05$; $^{**}p<0.008$

Intriguingly, mice with hepatocyte-specific Timp3 overexpression (AlbT3) were also largely resistant to DEN-induced hepatocarcinogenesis during obesity [13]. This is in line with the reduction in TIMP3 expression observed in the majority of human solid cancers [28, 29]. It can be speculated that in AlbT3 mice, in which Timp3 is overexpressed in hepatocyte cells, the tumor prevention may be associated with a direct effect of Timp3 on specific signaling pathways related to tumor development in hepatocyte cells. On the other hand, in Timp3$^{-/-}$ mice the protective effects may be ascribed to a reduction in cell growth and in regeneration due to the absence of Timp3 in both stromal and parenchymal cells.

We found that several critical genes involved in cell cycle control were down-regulated in Timp3 knockout mice upon DEN and HFD treatment, mostly related to G2/M transition. The strongest differential expression in our study was observed for H19, a long noncoding RNAs highly expressed in embryonic organs and absent or greatly reduced in most adult tissues [30]. Most studies have indicated that H19 is associated with cancer development. However, its reported functional mechanisms vary among cancer types [31]. Interestingly, H19 expression was significantly down-regulated in the myocardium of diabetic rats and in cultured neonatal rat cardiomyocytes grown in high-glucose conditions [32]. Moreover, in cultured human chondrocytes, inflammatory mediators such as IL-1β and TNF-α induced stimulus resulting in a decrease in H19 levels [33]. Modulation of Timp3 expression was identified as a common bond between glucose

intolerance and inflammation [34]. It can be speculated that environmental and genetic factors might cooperate in a context of HCC during obesity, resulting in the reduction in H19 expression also in liver. In the present study, H19 and miR-675 levels were co-regulated, suggesting that the microRNA might represent the effector for the H19 action in liver during tumorigenesis. miR-675 has been found to be a negative regulator of p53 [20]. Consistently, we have found, in liver 30 weeks post-DEN treatment, an increase in p53 protein expression in the absence of Timp3 in both lean and obese mice. In the context of DNA damage, p53 represented a crucial tumor suppressor, acting through different mechanisms including senescence or apoptosis [35]. Induction of p53 affects many aspects of cell cycle regulation through the transcriptional repression of several key genes, including CcnA2, Plk1, CcnB2, Cdk1, CDC20 and antiapoptotic survivin (BIRC5) [21]. Interestingly, expression of all these genes was reduced in Timp3$^{-/-}$ mice. However, p53 expression was induced during obesity in different tissues, and its inhibition increased insulin sensitivity and prevented hepatosteatosis and fat accumulation [36–38]. The evidence that DEN-treated Timp3 null mice showed high levels of p53 protein in both normal and HFD conditions, led us to hypothesize a potential contribution of Timp3 knockout in p53 regulation. However, how p53 is activated in response to HFD treatment is not fully understood and an additional mechanism involving Timp3, independent of H19/miR-675 pathway, should be further explored. In this study, we show that p53 increase is associated, under diet-induced obesity, with the down-regulation of FoxM1 and several FoxM1 targets. FoxM1 is a member of the Forkhead superfamily of transcription factors which regulates many G2/M-specific genes and which is overexpressed in a multitude of solid tumors [39–41]. In recent years, numerous studies have reported that FoxM1 is playing a crucial role in the negative regulation of the senescence program [42] and in HFD conditions H19 up-regulation has been found to up-regulate FoxM1: expression [43]. Therefore, in our HCC model, inhibition of Timp3 during obesity might induce cell cycle arrest at G2/M phase via repressing FoxM1 transcriptional activity through H19/miR-675/p53 pathway. The key mechanism of p53-mediated cell cycle arrest is represented by a transcriptional down-regulation of many cell cycle genes. The Cdc2–cyclin B1 complex is pivotal in regulating the G_2/M-phase transition and mitosis [39]. We observed a significant decrease in the expression level of cyclin B1 and CDC2 in tumors derived from Timp3$^{-/-}$ mice, suggesting, at least in part, an involvement in G_2/M-phase arrest. Moreover, FoxM1: represents a master regulator of cell cycle progression. Deregulated FOXM1 perturbs the timely and coordinated transition through the cell cycle, leading to a loss of checkpoint control in G1/S and G2/M [44]. Moreover, several key mitotic regulators significantly reduced in Timp3$^{-/-}$ mice, such as PLK1, Aurora B kinase, cyclin B and CENPF, are under transcriptional control of FoxM1:

Repression of FoxM1 oncogenic targets such as Aurka might lead to inhibition of p53 protein stability and transcriptional activity [45]. Our study has some limitations including that given the complexity of the protocol we could not assess the effect of DEN/HFD interaction at time points earlier than 32 weeks.

In conclusion, we observed a bimodal effect of the loss of Timp3 in a model of obesity-related hepatocellular carcinoma which, though reduced in number and size, showed features associated with non-alcoholic steatohepatitis.

Acknowledgements This manuscript was in part funded by Associazione Italiana per la Ricerca sul Cancro (Grant AIRC IG-13163), MIUR PRIN 2015MPESJS_004 and Fondazione Roma NCD 2014 to M.F., Fondazione Roma NCD 2014 and EFSD/Boehringer Ingelheim 2017 to R.M. Horizon 2020 (Grant MADIA 732678), MoDiag Grant and Regione Lazio, Bando Life 2014–2020 to M.D. and I.A.

Compliance with ethical standards

Ethical standard The handling of mice and experimental procedures were conducted in accordance with experimental animal guidelines. Animal studies were approved by the University of Tor Vergata Animal Care and Use Committee.

Conflict of interest The authors declare that they have no conflict of interest.

Informed consent For this type of study informed consent is not required.

References

1. Agosti P, Sabbà C, Mazzocca A (2018) Emerging metabolic risk factors in hepatocellular carcinoma and their influence on the liver microenvironment. Biochim Biophys Acta Mol Basis Dis 1864:607–617. https://doi.org/10.1016/j.bbadis.2017.11.026
2. Lonardo A, Lugari S, Ballestri S, Nascimbeni F, Baldelli E, Maurantonio M (2019) A round trip from nonalcoholic fatty liver disease to diabetes: molecular targets to the rescue? Acta Diabetol 56:385–396. https://doi.org/10.1007/s00592-018-1266-0
3. Yang WS, Chen PC, Lin HJ et al (2017) Association between type 2 diabetes and cancer incidence in Taiwan: data from a prospective community-based cohort study. Acta Diabetol 54:455–461. https://doi.org/10.1007/s00592-017-0966-1
4. Federici M, Hribal ML, Menghini R et al (2005) Timp3 deficiency in insulin receptor haploinsufficient mice promotes diabetes and vascular inflammation via increased TNF-alpha. J Clin Invest 115:3494–3505. https://doi.org/10.1172/JCI26052
5. Menghini R, Menini S, Amoruso R et al (2009) Tissue inhibitor of metalloproteinase 3 deficiency causes hepatic steatosis and adipose tissue inflammation in mice. Gastroenterology 136:663–672. e4. https://doi.org/10.1053/j.gastro.2008.10.079

6. Menghini R, Fiorentino L, Casagrande V, Lauro R, Federici M (2013) The role of ADAM17 in metabolic inflammation. Atherosclerosis 228:12–17. https://doi.org/10.1016/j.atherosclerosis.2013.01.024
7. Fiorentino L, Vivanti A, Cavalera M et al (2010) Increased tumor necrosis factor alpha-converting enzyme activity induces insulin resistance and hepatosteatosis in mice. Hepatology 51:103–110. https://doi.org/10.1002/hep.23250
8. Anand-Apte B, Bao L, Smith R et al (1996) A review of tissue inhibitor of metalloproteinases-3(TIMP-3) and experimental analysis of its effect on primary tumor growth. Biochem Cell Biol 74:853–862
9. Kallio JP, Hopkins-Donaldson S, Baker AH, Kähäri VM (2011) TIMP-3 promotes apoptosis in non adherent small cell lung carcinoma cells lacking functional death receptor pathway. Int J Cancer 128:991–996. https://doi.org/10.1002/ijc.25404
10. Chavey C, Mari B, Monthouel MN et al (2003) Matrix metalloproteinases are differentially expressed in adipose tissue during obesity and modulate adipocyte differentiation. J Biol Chem 278:11888–11896. https://doi.org/10.1074/jbc.M209196200
11. Cardellini M, Menghini R, Martelli E et al (2009) TIMP3 is reduced in atherosclerotic plaques from subjects with type 2 diabetes and increased by SirT1. Diabetes 58:2396–2401. https://doi.org/10.2337/db09-0280
12. Lee JS, Chu IS, Mikaelyan A et al (2004) Application of comparative functional genomics to identify best-fit mouse models to study human cancer. Nat Genet 36:1306–1311. https://doi.org/10.1038/ng1481
13. Casagrande V, Mauriello A, Bischetti S, Mavilio M, Federici M, Menghini R (2017) Hepatocyte specific TIMP3 expression prevents diet dependent fatty liver disease and hepatocellular carcinoma. Sci Rep 7:6747. https://doi.org/10.1038/s41598-017-06439-x
14. Defamie V, Sanchez O, Murthy A, Khokha R (2015) TIMP3 controls cell fate to confer hepatocellular carcinoma resistance. Oncogene 34:4098–4108. https://doi.org/10.1038/onc.2014.339
15. Duan T, Sun W, Zhang M et al (2017) Dietary restriction protects against diethylnitrosamine-induced hepatocellular tumorigenesis by restoring the disturbed gene expression profile. Sci Rep 7:43745. https://doi.org/10.1038/srep43745
16. Rossi C, Marzano V, Consalvo A et al (2018) Proteomic and metabolomic characterization of streptozotocin-induced diabetic nephropathy in TIMP3-deficient mice. Acta Diabetol 55:121–129. https://doi.org/10.1007/s00592-017-1074-y
17. Menghini R, Casagrande V, Marino A et al (2014) MiR-216a: a link between endothelial dysfunction and autophagy. Cell Death Dis 5:e1029. https://doi.org/10.1038/cddis.2013.556
18. Hill-Baskin AE, Markiewski MM, Buchner DA et al (2009) Diet-induced hepatocellular carcinoma in genetically predisposed mice. Hum Mol Genet 18:2975–2988. https://doi.org/10.1093/hmg/ddp236
19. He D, Wang J, Zhang C et al (2015) Down-regulation of miR-675-5p contributes to tumor progression and development by targeting pro-tumorigenic GPR55 in non-small cell lung cancer. Mol Cancer 14:73. https://doi.org/10.1186/s12943-015-0342-0
20. Liu C, Chen Z, Fang J, Xu A, Zhang W, Wang Z (2016) H19-derived miR-675 contributes to bladder cancer cell proliferation by regulating p53 activation. Tumour Biol 37:263–270. https://doi.org/10.1007/s13277-015-3779-2
21. Engeland K (2018) Cell cycle arrest through indirect transcriptional repression by p53: I have a DREAM. Cell Death Differ 25:114–132. https://doi.org/10.1038/cdd.2017.172
22. Liu X, Zhou Y, Liu X et al (2014) MPHOSPH1: a potential therapeutic target for hepatocellular carcinoma. Cancer Res 74:6623–6634. https://doi.org/10.1158/0008-5472.CAN-14-1279
23. Barsotti AM, Prives C (2009) Pro-proliferative FoxM1 is a target of p53-mediated repression. Oncogene 28:4295–4305. https://doi.org/10.1038/onc.2009.282
24. Gan L, Liu Z, Sun C (2018) Obesity linking to hepatocellular carcinoma: a global view. Biochim Biophys Acta Rev Cancer 1869:97–102. https://doi.org/10.1016/j.bbcan.2017.12.006
25. Elsegood CL, Tirnitz-Parker JE, Olynyk JK, Yeoh GC (2017) Immune checkpoint inhibition: prospects for prevention and therapy of hepatocellular carcinoma. Clin Transl Immunol 6:e161. https://doi.org/10.1038/cti.2017.47
26. Bachman KE, Herman JG, Corn PG et al (1999) Methylation-associated silencing of the tissue inhibitor of metalloproteinase-3 gene suggest a suppressor role in kidney, brain, and other human cancers. Cancer Res 59:798–802
27. Gill SE, Gharib SA, Bench EM et al (2013) Tissue inhibitor of metalloproteinases-3 moderates the proinflammatory status of macrophages. Am J Respir Cell Mol Biol 49:768–777. https://doi.org/10.1165/rcmb.2012-0377OC
28. Masson D, Rioux-Leclercq N, Fergelot P et al (2010) Loss of expression of TIMP3 in clear cell renal cell carcinoma. Eur J Cancer 46:1430–1437. https://doi.org/10.1016/j.ejca.2010.01.009
29. Nakamura M, Ishida E, Shimada K et al (2005) Frequent LOH on 22q12.3 and TIMP-3 inactivation occur in the progression to secondary glioblastomas. Lab Invest 85:165–175. https://doi.org/10.1038/labinvest.3700223
30. Pope C, Mishra S, Russell J, Zhou Q, Zhong XB (2017) Targeting H19, an imprinted long non-coding RNA, in hepatic functions and liver diseases. Diseases 5:E11. https://doi.org/10.3390/diseases5010011
31. Yoshimizu T, Miroglio A, Ripoche MA et al (2008) The H19 locus acts in vivo as a tumor suppressor. Proc Natl Acad Sci USA 105:12417–12422. https://doi.org/10.1073/pnas.0801540105
32. Li X, Wang H, Yao B, Xu W, Chen J, Zhou X (2016) lncRNA H19/miR-675 axis regulates cardiomyocyte apoptosis by targeting VDAC1 in diabetic cardiomyopathy. Sci Rep 6:36340. https://doi.org/10.1038/srep36340
33. Steck E, Boeuf S, Gabler J et al (2012) Regulation of H19 and its encoded microRNA-675 in osteoarthritis and under anabolic and catabolic in vitro conditions. J Mol Med 90:1185–1195. https://doi.org/10.1007/s00109-012-0895-y
34. Menghini R, Casagrande V, Menini S et al (2012) TIMP3 overexpression in macrophages protects from insulin resistance, adipose inflammation, and nonalcoholic fatty liver disease in mice. Diabetes 61:454–462. https://doi.org/10.2337/db11-0613
35. Vousden KH, Prives C (2009) Blinded by the light: the growing complexity of p53. Cell 137:413–431. https://doi.org/10.1016/j.cell.2009.04.037
36. Derdak Z, Villegas KA, Harb R, Wu AM, Sousa A, Wands JR (2013) Inhibition of p53 attenuates steatosis and liver injury in a mouse model of non-alcoholic fatty liver disease. J Hepatol 58:785–791. https://doi.org/10.1016/j.jhep.2012.11.042
37. Minamino T, Orimo M, Shimizu I et al (2009) A crucial role for adipose tissue p53 in the regulation of insulin resistance. Nat Med 15:1082–1087. https://doi.org/10.1038/nm.2014
38. Yokoyama M, Okada S, Nakagomi A et al (2014) Inhibition of endothelial p53 improves metabolic abnormalities related to dietary obesity. Cell Rep 7:1691–1703. https://doi.org/10.1016/j.celrep.2014.04.046
39. Taylor WR, Stark GR (2001) Regulation of the G2/M transition by p53. Oncogene 20:1803–1815. https://doi.org/10.1038/sj.onc.1204252
40. Laoukili J, Stahl M, Medema RH (2007) FoxM1: at the crossroads of ageing and cancer. Biochim Biophys Acta 1775:92–102. https://doi.org/10.1016/j.bbcan.2006.08.006
41. Pilarsky C, Wenzig M, Specht T, Saeger HD, Grutzmann R (2004) Identification and validation of commonly overexpressed genes

in solid tumors by comparison of microarray data. Neoplasia 6:744–750. https://doi.org/10.1593/neo.04277
42. Alvarez-Fernandez M, Medema RH (2013) Novel functions of FoxM1: from molecular mechanisms to cancer therapy. Front Oncol 3:30. https://doi.org/10.3389/fonc.2013.00030
43. Wang SH, Ma F, Tang ZH et al (2016) Long non-coding RNA H19 regulates FOXM1 expression by competitively binding endogenous miR-342-3p in gallbladder cancer. J Exp Clin Cancer Res 35:160. https://doi.org/10.1186/s13046-016-0436-6
44. Lam EW, Brosens JJ, Gomes AR, Koo CY (2013) Forkhead box proteins: tuning forks for transcriptional harmony. Nat Rev Cancer 13:482–495. https://doi.org/10.1038/nrc3539
45. Pérez de Castro I, Aguirre-Portolés C, Fernández-Miranda G et al (2013) Requirements for Aurora-A in tissue regeneration and tumor development in adult mammals. Cancer Res 73:6804–6815. https://doi.org/10.1158/0008-5472.CAN-13-0586